

December 2, 2005

MSU-HEP-051205
CTEQ-051205

Parton Distributions and the Strong Coupling Strength α_s

J. Pumplin, A. Belyeav, J. Huston, D. Stump, W.K. Tung

Department of Physics and Astronomy
Michigan State University, E. Lansing, MI 48824

We study the global analysis for parton distributions as a function of the QCD strong coupling strength α_s , and present a new series of distributions that span the range $0.110 < \alpha_s(m_Z) < 0.128$. We use these distributions to explore the correlation between α_s and the gluon distribution; the viability of global analysis as a method to measure α_s ; and the dependence on α_s of predictions for W , Z , inclusive jet, and Higgs boson production cross sections at the Tevatron and the LHC. In addition to the gg process that dominates Higgs production in the Standard Model, we also consider production from $b\bar{b}$, which can be important scenarios such as MSSM.

Contents

1	Introduction	1
2	Definitions for $\alpha_s(\mu)$	2
3	The CTEQ6 α_s series of global fits	3
4	The gluon distribution and α_s	4
5	Determining α_s from global analysis?	5
6	Dependence on α_s of predictions for physical cross sections	8
6.1	W and Z production	8
6.2	Inclusive Jets	11
6.3	Higgs boson cross section in SM and MSSM	12
7	Conclusion	14

1 Introduction

The theory of Quantum Chromodynamics (QCD) depends on the fundamental gauge coupling strength α_s and suitably defined quark mass parameters m_f . For applications to hard scattering processes with hadrons in the initial state, we also need the universal parton distribution functions (PDFs) that characterize the partonic structure of those hadrons. These PDFs are determined by global QCD analysis, using input from a variety of well-established experimental measurements.

In the standard CTEQ analysis [1], the focus is on determining the parton distribution functions. The value of $\alpha_s(m_Z)$ is fixed at the world average value, which is dominantly based on dedicated measurements such as those from LEP. The reason for fixing $\alpha_s(m_Z)$ is that it can be determined more cleanly and reliably in processes that are free of the complications of hadronic structure.

However, the interplay between the coupling strength α_s and strong dynamics is an interesting subject in itself. Many attempts have been made to extract $\alpha_s(m_Z)$ from individual experiments at HERA and at the Tevatron, and from combined analyses of different hadronic experiments. For such studies, as well as to assess the additional uncertainty in predictions caused by the uncertainty in $\alpha_s(m_Z)$, it is important to have PDF sets available that are based on a range of different values for α_s . The purpose of this paper is to fill that need.

We provide here a series of PDF sets that span a range of coupling strengths from $\alpha_s(m_Z) = 0.110$ to 0.128 . These PDFs extend and update the CTEQ6 global analysis [1]. Complementary to the physics probed in [1], we will discuss several issues related

to the dependence on the input value of α_s : the correlation between α_s and the parton distributions—particularly the gluon distribution; the viability of using global analysis of hadronic processes to measure α_s ; and the dependence on α_s of physics predictions for W , Z , jet, and Higgs boson cross sections at the Tevatron and the LHC.

We provide two different sets of fits—CTEQ6A and CTEQ6B—corresponding to two different common definitions for $\alpha_s(\mu)$ that are defined in the next Section.

2 Definitions for $\alpha_s(\mu)$

The dependence of the QCD coupling strength $\alpha_s(\mu)$ on the momentum scale μ is governed by the renormalization group equation (RGE), which in next-to-leading order (NLO) perturbation theory is

$$\mu d\alpha/d\mu = c_1\alpha^2 + c_2\alpha^3, \quad (1)$$

where $c_1 = -\beta_0/2\pi$ with $\beta_0 = 11 - (2/3)n_f$, and $c_2 = -\beta_1/8\pi^2$ with $\beta_1 = 102 - (38/3)n_f$. The coefficients are functions of the number of active quark-parton flavors n_f , an integer variable. The number n_f changes with μ , increasing by 1 as μ passes the mass m_f of each quark flavor. Nonetheless, it is known that at NLO, the function $\alpha_s(\mu)$ is a *continuous* function of μ at each quark mass threshold, provided the matching point is chosen at $\mu = m_f$: The $(n_f - 1)$ -flavor renormalization scheme for $\mu < m_f$ joins continuously with the n_f -flavor scheme for $\mu > m_f$. The solution to Eq. (1) therefore depends on a single integration constant, which is the fundamental coupling strength parameter of QCD that is conveniently characterized by $\alpha_s(m_Z)$.

Since Eq. (1) is truncated at $\mathcal{O}(\alpha^3)$, there are infinitely many definitions of $\alpha_s(\mu)$ that are formally equivalent because they differ only in higher orders of the perturbative expansion. Two conventional choices are often used in QCD phenomenology:

- **Def. A.** The original NLO definition [2] is given by

$$\alpha_s(\mu) = c_3 [1 - c_4 \ln(L)/L]/L, \quad (2)$$

where $L = \ln(\mu^2/\Lambda^2)$, $c_3 = -2/c_1$, and $c_4 = -2c_2/c_1^2$. The parameter Λ depends on n_f , and hence takes on different values Λ_{n_f} when μ crosses each quark mass threshold. Previous CTEQ global analyses have all used this definition for the running coupling.

- **Def. B.** An alternative is to solve the truncated RGE (1) exactly. The publicly available evolution program QCDNUM [3], and many HERA analyses use this definition.

We have shown previously [4] that these two forms are numerically quite similar in the region $Q > 2\text{ GeV}$ where we fit data. In the following, we present results based on both definitions,¹

¹The form used for PDF fitting by MRST [5] is different from both of these definitions, but is numerically very close to Def. B [4]. The definition used by the Particle Data Group lies between Def. A and Def. B.

3 The CTEQ6 α_s series of global fits

To study the interplay between the strong coupling strength α_s and the PDFs, one can either perform a fully global QCD fit by varying α_s and the PDF parameters simultaneously to examine the neighborhood of the overall global minimum in χ^2 ; or one can perform a series of fits to the PDF parameters at various fixed values for α_s . We have explored both of these approaches, but concentrate here on the second approach since it is most convenient for general collider physics applications. We therefore present here a series of PDFs—the CTEQ6 α_s -series. Some of their physical implications are discussed in Sec. 6. Earlier PDF fits with a range of $\alpha_s(m_Z)$ have been obtained in [6].

The PDFs in the new series were obtained for 10 values of $\alpha_s(m_Z) = 0.110, 0.112, \dots, 0.128$, where $m_Z = 91.188$ GeV is assumed. The theoretical assumptions and functional parametrization of these PDFs at the initial momentum scale $\mu_0 = 1.3$ GeV are the same as in the previous CTEQ6 analyses [1, 7]. The experimental input is slightly updated.² These PDF sets are designated as CTEQ6A110, \dots , CTEQ6A128 using Def. A for α_s ; and CTEQ6B110, \dots , CTEQ6B128 using Def. B for α_s . The central fits CTEQ6A118 and CTEQ6B118, with $\alpha_s(m_Z) = 0.118$, are nearly the same as CTEQ6M or CTEQ6.1M, but are not identical to either due to minor updates in experimental input, and in the case of CTEQ6B118 the different definition for α_s . All 20 of these PDF sets will give very similar physical predictions in most applications.

Figure 1 shows the quality of the global fits, as measured by the overall χ^2 for the fit to ~ 2000 data points, as a function of $\alpha_s(m_Z)$.³ The two curves, both approximately parabolic, are smooth interpolations of the above series of fits. The curves are very similar, with the Def. A curve being slightly narrower and slightly farther to the left because Def. A has a slightly more rapid variation of $\alpha_s(\mu)$ with μ . The minima of these curves are at $\alpha_s(m_Z) = 0.1172$ and 0.1176 , very close to the current world average (0.1187 ± 0.0020) [17] and very close to the value 0.1180 adopted in CTEQ6M and CTEQ6.1M. This similarity in α_s is an impressive demonstration of consistency between QCD theory and experiment, since our analysis is based on hard scattering data with hadronic initial states, while the determination of the world average value for α_s comes mainly from totally different physical processes such as e^+e^- annihilation, τ -decay, and even lattice gauge theory calculations with quarkonium spectra as input.

Note that the range of $\alpha_s(m_Z)$ covered by the CTEQ6A/B series is much wider than the currently accepted 1σ error range of the world average quoted above. We explore this extended range because the lowest and highest values ($0.110, 0.128$) represent outlying values that have been obtained by some individual experiments that are included in the world average. The fits with extreme values of $\alpha_s(m_Z)$ will be useful for some specialized applications. In plots shown later in this paper, we show almost all of this range, but reduce it to

²The input experimental data consist of BCDMS [8], H1 [9], ZEUS [10], NMC [11], CCFR [12], E866 [13], CDF W-lepton asymmetry [14], CDF jet [15] and D0 jet [16].

³This figure is an improved version of one appearing in [4].

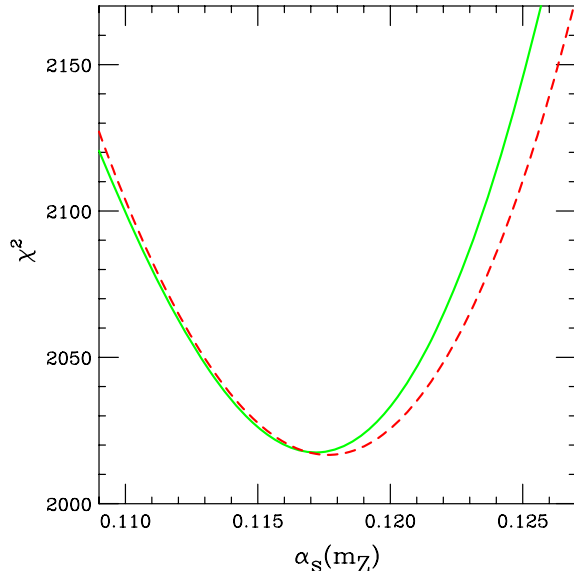


Figure 1: The overall goodness-of-fit measure χ^2 for global fits vs. $\alpha_s(m_Z)$, using Def. A (solid curve) and Def. B (dashed curve).

0.110 to 0.126 to be symmetric about the CTEQ6 value of 0.118. Note that χ^2 increases by ~ 100 above its minimum at the extremes of this reduced range, which makes it consistent with a 90% confidence range for the global fit according to results of our previous analyses. However, the reader must keep in mind that this range of $\alpha_s(m_Z)$ is larger by a factor of ~ 4 than the uncertainty range corresponding to a “ 1σ ” error band based on the world average data.

4 The gluon distribution and α_s

The gluon distribution is strongly correlated with α_s in the global QCD analysis. Gluon distributions $g(x, \mu)$ from the α_s -series PDFs are shown in Fig. 2(a) for $\mu = 3.162$ GeV. For clarity of display over the significant range in x , the horizontal axis is scaled as $x^{1/3}$ and the vertical axis is weighted by $x^{3/2}$.

For comparison, Fig. 2(b) shows the uncertainty band (shaded area) of the gluon distribution at a fixed value $\alpha_s(m_Z) = 0.118$, obtained by the Hessian method [18], using the 40 eigenvector basis sets of CTEQ6.1 [7]. The CTEQ6.1M (solid) and the new CTEQ6A118 (dashed) distributions, which are very similar, are also shown in Fig. 2(b). The two figures are combined in Fig. 2(c), where, in order to highlight the differences, the results are shown as ratios to the CTEQ6.1M distribution.

There is a clear systematic trend in the α_s -series for the gluon distribution function. Fits with larger $\alpha_s(m_Z)$ have a gluon component that is weaker at small x and stronger at large x . The behavior at small x results from the fact that every occurrence of $g(x, \mu)$ in a

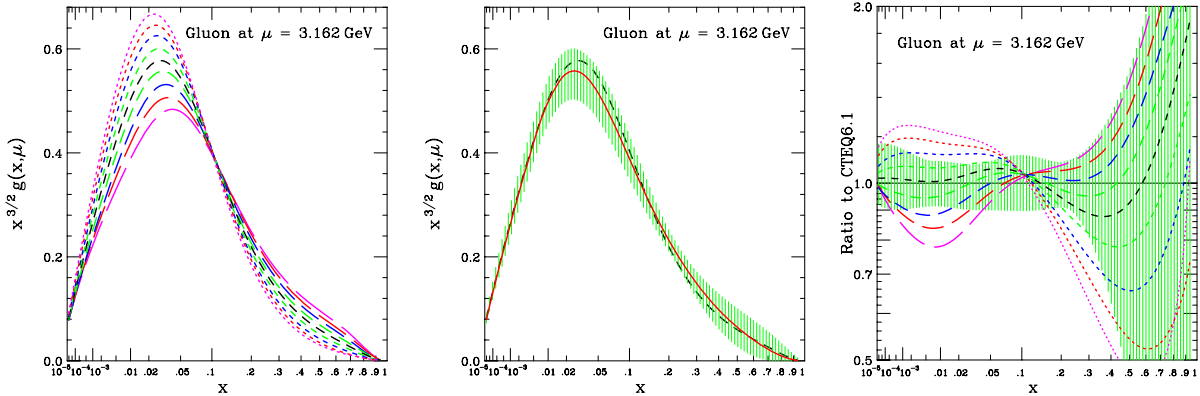


Figure 2: (a) Gluon distributions for $\alpha_s(m_Z) = 0.110$ (short dash), \dots , 0.126 (long dash), using Def. A for α_s ; (b) Gluon distribution from CTEQ6.1M (solid), $\alpha_s(m_Z) = 0.118$ (dashed), and uncertainty band from CTEQ6.1 eigenvector sets (shaded); (c) Both plots combined in ratio form.

cross section formula is accompanied by a factor of α_s , so when α_s is made larger, the gluon distribution becomes smaller in order to maintain agreement with the large amount of data at small x . The behavior at large x , where there is little direct constraint from experiment, is dictated by the momentum sum rule: the momentum fraction carried by gluon + quarks must be equal to 1, and the momentum carried by quarks is tightly constrained by DIS data.

Another feature seen in Fig. 2 is that the gluon distributions for different $\alpha_s(m_Z)$ values all nearly intersect at a common value of $x \approx 0.1$. This occurs simply because the function $g(x, \mu, \alpha_s(m_Z))$ has an approximately linear dependence on the parameter $\alpha_s(m_Z)$.

Comparing the range of variation of $g(x, \mu)$ due to the variation of α_s , to the uncertainty range due to other sources of error, we see that the two are comparable throughout most of the domain in x . The *combined* uncertainty on the gluon distribution is therefore somewhat larger than the previously published uncertainties, which were obtained at fixed $\alpha_s(m_Z)$.

We remark that the variation of quark distributions with $\alpha_s(m_Z)$ (not shown) is much smaller than that of the gluon distribution, and is also small compared to the PDF uncertainty due to other sources.

5 Determining α_s from global analysis?

Can one determine the coupling strength α_s from a global QCD fit with hadronic processes? The obvious answer is yes, since one can simply treat the parameter $\alpha_s(m_Z)$ as one of the fitting parameters. We see from the minima in Fig. 1 that a “best fit” value of $\alpha_s(m_Z)$ is around 0.1174, which is very close to the world average. The difficult question is, however, how much uncertainty should be assigned to this measurement? The answer to that question will determine whether this method is competitive with measurements that are independent of the complications of hadron partonic structure. The fact that the value of $\alpha_s(m_Z)$ in global

analysis is strongly correlated with the rather uncertain gluon distribution, as discussed in the previous section, suggests that caution is needed.

Referring again to Fig. 1, the range of $\alpha_s(m_Z)$ (horizontal axis) allowed by global analysis based on minimization of χ^2 , is set by the increase of χ^2 (vertical axis) above the global minimum that we allow. We refer to the allowed increase of χ^2 as the *tolerance*, $\Delta\chi^2$. Recent studies of uncertainties of PDFs by various global analysis groups [1, 5, 19] have concluded that a reasonable tolerance $\Delta\chi^2$ must be rather large, in the range 50 – 100 for the ~ 2000 points in present-day data sets, to define an approximate 90% confidence range. Making the specific choice $\Delta\chi^2 = 75$, the corresponding range of $\alpha_s(m_Z)$ is from 0.1104 to 0.1237. Assuming that range to be the 90% confidence range for a gaussian distribution, this corresponds to $\alpha_s(m_Z) = 0.1171 \pm 0.0040$ for a “ 1σ ” error range. Thus the measurement of $\alpha_s(m_Z)$ provided by PDF fitting agrees very well with the Particle Data Group world average of 0.1187 ± 0.0020 [17], but has approximately twice the uncertainty.

We can gain some insight on how α_s is constrained in the global QCD analysis by examining the dependence on $\alpha_s(m_Z)$ of the χ^2 values for each individual experiment that contributes to that analysis. These χ^2 “parabolas” are shown in Fig. 3. The curves represent smooth interpolations of the results from the 10 fits in the CTEQA α_s -series. The horizontal axis is $\alpha_s(m_Z)$. The vertical axis in each graph is the χ^2 value *per data point* in the fit to that experiment.

It is apparent in Fig. 3 that the sensitivities of the various experiments to α_s vary greatly. Some of the curves are approximately parabolic with a minimum within the range probed; others merely constrain the value of $\alpha_s(m_Z)$ from above or below. The global minimum seen in Fig. 1 is due to the combined constraints of all the experiments. Since different experiments prefer different values of $\alpha_s(m_Z)$, which are not always consistent with each other if strict statistical criteria are applied,⁴ the global minimum represents a compromise that is difficult to interpret as a “measurement” in the traditional sense. In particular, there is no clear way to assign a statistically meaningful error to the measurement. Rather, the error is dominated by systematic effects that can only be estimated.

So Fig. 3 demonstrates an important aspect of global analysis. The measurement of $\alpha_s(m_Z)$ by an individual experiment, from a hard-scattering process with initial-state hadrons, may nominally yield a narrow range of statistical uncertainty; examples are [20] and [21]. However, the influence of other experimental input can have a significant impact on the eventual determination of $\alpha_s(m_Z)$. The full effects due to hadronic degrees of freedom, such as the uncertainties of the gluon distribution, are impossible to include in the error analysis of any single experiment.

⁴We should point out that the χ^2 curves shown in Fig. 3 are not to be compared directly to those obtained by individual experiments in their respective determinations of α_s . Points on our curves correspond to χ^2 values evaluated using constrained fits to the full global data set, not just to the data of a single experiment. Only the general trends of the dependence on α_s should be similar.

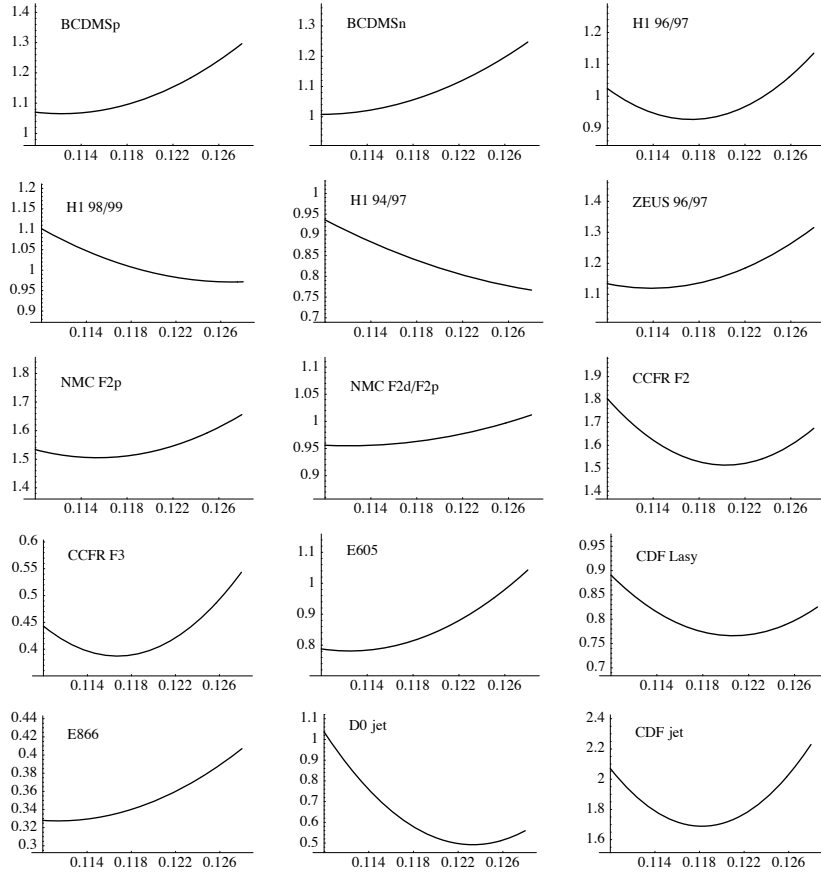


Figure 3: The dependence on $\alpha_s(m_Z)$, for the χ^2 values (per data point) of the individual experiments that are included in the global analysis.

6 Dependence on α_s of predictions for physical cross sections

Here we present predictions for several important processes at the Tevatron ($p\bar{p}$ at $\sqrt{s} = 1.96$ TeV) and the LHC (pp at $\sqrt{s} = 14$ TeV). The results show how the uncertainty in α_s propagates to uncertainties in the predictions. Conversely, the results show to what extent accurate measurements of these cross sections could be used to constrain α_s .

We show predictions using the Def. A form for α_s . Results for the Def. B form are very similar. The figures show the variation of the predictions for the range of $\alpha_s(m_Z)$ from 0.110 to 0.126. We again remind the reader that this range is much larger than the actual uncertainty of $\alpha_s(m_Z)$; i.e., the full variation of the physical prediction shown in the figure extends beyond the uncertainty from α_s . The shaded region in each figure shows the range of uncertainty due to sources other than α_s , as calculated from the eigenvector basis sets of CTEQ6.1 using the Hessian method [7, 18].

6.1 W and Z production

Figure 4 shows the cross section for W^- production at the Tevatron. W^+ production is identical except for $y \rightarrow -y$. The left plot shows $d\sigma/dy_W$ versus the W rapidity y_W . The right plot shows the difference from the prediction of CTEQ6.1, which has $\alpha_s(m_Z) = 0.118$. The curves are the CTEQ6A α_s -series, and the shaded band is the range of uncertainty for fixed $\alpha_s(m_Z)$ calculated using the Hessian method. For this process, the Hessian uncertainty range is about $\pm 5\%$ of the central prediction. The variation with α_s is smaller, on the order of $\pm 2\%$ even for the rather extreme range of $\alpha_s(m_Z)$ from 0.110 to 0.126.

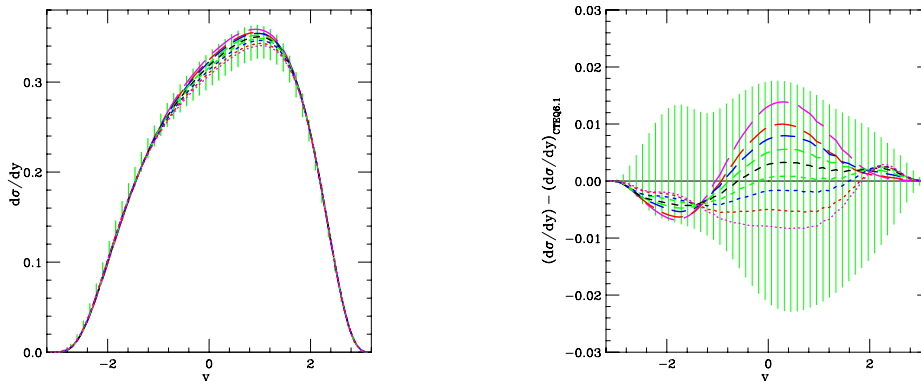


Figure 4: (a) Cross section $d\sigma/dy_W$ for W^- production at the Tevatron. (b) Same cross section with the CTEQ6.1 prediction subtracted. The curves are for $\alpha_s(m_Z) = 0.110$ (short dash), \dots , 0.126 (long dash) in Fig. 2.

Figure 5 shows the cross section $d\sigma/dy_Z$ for Z^0 production at the Tevatron. Again the Hessian uncertainty range is $\sim \pm 5\%$ and again the variation with $\alpha_s(m_Z)$ is again $\sim \pm 2\%$

for the rather extreme range of α_s .

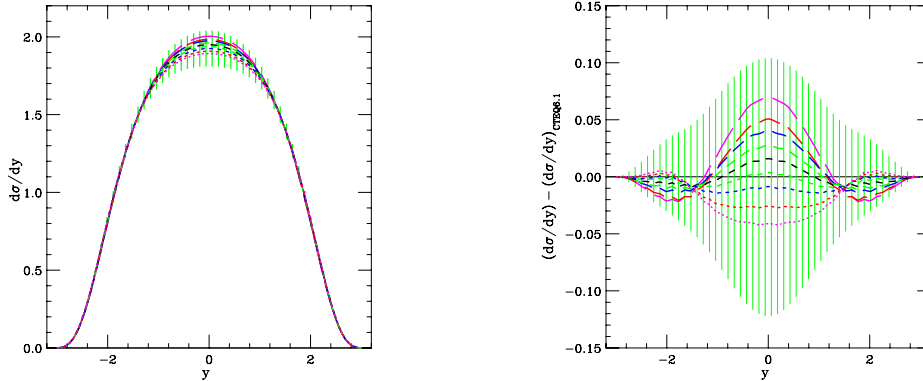


Figure 5: (a) Production of Z^0 at the Tevatron; (b) Same process with the CTEQ6.1 prediction subtracted.

Figure 6 shows the cross section for W^- production at the LHC. The Hessian uncertainty range is again of order $\pm 5\%$, but the variation with α_s is larger than for the Tevatron, of order $\pm 5\%$ for the large range of $\alpha_s(m_Z)$ that is shown. Figure 7 shows the process of W^+ production at the LHC; it has a larger cross section at large rapidity (because $u(x) > d(x)$ for the valence quarks) and a similar range of uncertainty in the prediction. The difference between the central dashed curve and a horizontal line in Figs. 6 and 7 shows the effect of updates in the fitting between CTEQ6.1 and CTEQ6A118—the change is well within the estimated PDF errors.

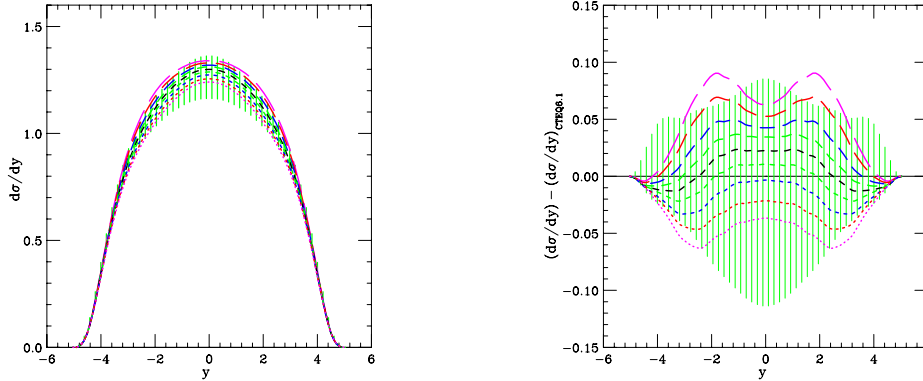


Figure 6: (a) Production of W^- at the LHC; (b) Same process with the CTEQ6.1 prediction subtracted.

The cross section for W production at the LHC is closely related to the gluon distribution, since the leading-order process in proton-proton collisions is $u + \bar{d} \rightarrow W^+$, which involves a sea quark, and sea quarks and the gluon are closely related at large μ by the evolution equations. (Proton-antiproton collisions at the Tevatron are different because both u and \bar{d} can be valence quarks—which causes the asymmetry in y that can be seen in Fig. 4.)

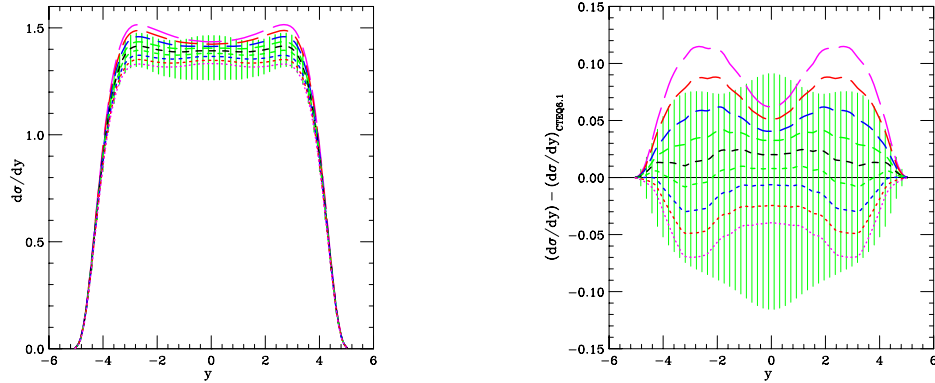


Figure 7: (a) Production of W^+ at the LHC. (b) Same process with the CTEQ6.1 prediction subtracted.

Also, the next-to-leading order process $u + g \rightarrow d + W^+$ involves an initial gluon directly. So the predictions for W production at the LHC depend on the rather uncertain gluon distribution function. The uncertainty of $g(x)$ is closely related to that of α_s as discussed in Sec. 4. Hence the Hessian uncertainty range and the variation with $\alpha_s(m_Z)$ are comparable in Figs. 6 and 7 as they are in Fig. 2.

6.2 Inclusive Jets

Figure 8(a) shows the α_s -dependence of the prediction for inclusive jet production in Run 2 at the Tevatron. We consider the cross section $d\sigma/dp_T$ for the CDF central rapidity cut $0.1 < |y| < 0.7$.

The α_s dependence is exhibited by plotting the ratio of the predicted cross section $d\sigma/dp_T$ to the prediction calculated using CTEQ6.1. The shaded region is the uncertainty range for fixed $\alpha_s(m_Z) = 0.118$ calculated from the eigenvector basis sets of the Hessian approach [7, 18].



Figure 8: Jet predictions for (a) Tevatron; and (b) LHC.

Figure 8(b) shows the α_s dependence of the cross section for inclusive jet production at the LHC for the rapidity range $|y| < 1$.

We remark that if we restrict the range of $\alpha_s(m_Z)$ to values from 0.115 to 0.120, then the uncertainty band due to the variation of α_s will be generally smaller than that due to the experimental input of the global analysis. In particular, the variation with α_s is much smaller than the uncertainty of the cross section for large p_T , which is dominated by the very uncertain gluon at large x .

6.3 Higgs boson cross section in SM and MSSM

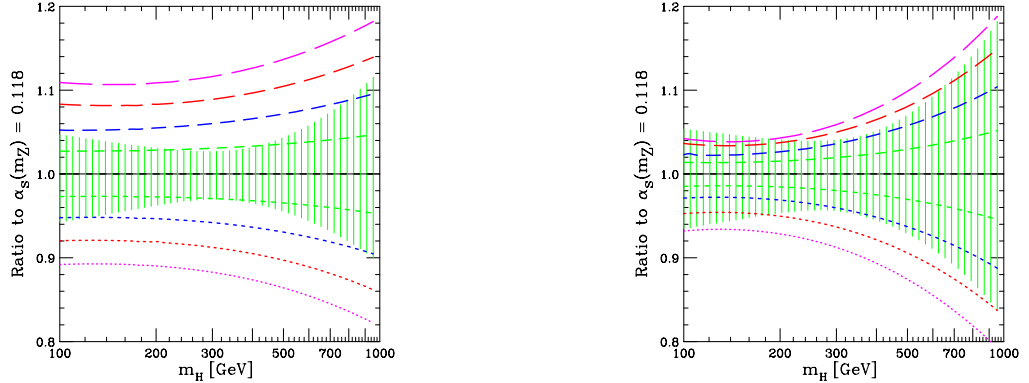


Figure 9: Uncertainty of predictions for Higgs boson production at LHC. (a) is for the SM and MSSM process $gg \rightarrow H$ via top triangle diagram. (b) is for the MSSM process $b\bar{b} \rightarrow H$. Curves (short dash to long dash) show ratio $\sigma_H(\alpha_s(m_Z))/\sigma_H(0.118)$ for $\alpha_s(m_Z) = 0.110, \dots, 0.126$. Shaded region shows the uncertainty at $\alpha_s(m_Z) = 0.118$ from other sources.

Figure 9 shows the uncertainty of the predicted cross section for Higgs boson production at the LHC as a function of Higgs mass. Figure 9(a) shows the uncertainty for the $gg \rightarrow H$ process, while Fig. 9(b) shows the uncertainty for the $b\bar{b} \rightarrow H$ mechanism. These cross sections were calculated at NLO using programs from [22, 23] and [24] respectively. Both of these processes play an important role in Higgs physics: in the Standard Model (SM), the gg process dominates over $b\bar{b}$; while in Supersymmetry and some other generic extensions of SM, the $b\bar{b} \rightarrow H$ process can be equally important or even dominant over $gg \rightarrow H$. The study of PDF uncertainties is important for both mechanisms of Higgs production.

The uncertainties based on the 40 eigenvector sets of CTEQ6.1 are shown as the shaded regions. These have been shown previously for $gg \rightarrow H$ [25] and for $b\bar{b} \rightarrow H$ [26]. These uncertainties are $gg \rightarrow H$ in comparison with $b\bar{b} \rightarrow H$ one are almost a factor of two smaller for sources different from α_s [27, 28].

Each Figure shows 9 curves corresponding to different α_s values from 0.110 to 0.126 with the 0.02 step from bottom to top. The central value of $\alpha_s = 0.118$ corresponds to the horizontal line with $\delta\sigma_{\alpha_s}^{PDF} = 0$.

It is very interesting to notice that $\delta\sigma^{PDF}$ and $\delta\sigma_{\alpha_s}^{PDF}$ are qualitatively different for $b\bar{b} \rightarrow H$ process as compared to $gg \rightarrow H$. Contrary to $\delta\sigma^{PDF}$, $\delta\sigma_{\alpha_s}^{PDF}$ is *about factor two larger* for $gg \rightarrow H$ in comparison with $b\bar{b} \rightarrow H$ production. If we restrict ourselves by $0.114 < \alpha_s < 0.122$ range, then one can clearly see that $\delta\sigma^{PDF} \lesssim \delta\sigma_{\alpha_s}^{PDF}$ for $b\bar{b} \rightarrow H$ process while $\delta\sigma^{PDF} > \delta\sigma_{\alpha_s}^{PDF}$ for $gg \rightarrow H$ production. Moreover in the region, where PDF uncertainties are minimal at $M_H \simeq 300$ GeV, for $gg \rightarrow H$ production $\delta\sigma_{\alpha_s}^{PDF}$ is twice as big as $\delta\sigma^{PDF}$. Therefore one concludes, that $\delta\sigma_{\alpha_s}^{PDF}$ is the dominant source of PDF uncertainties for $gg \rightarrow H$ production. One actually could expect the higher sensitivity of $gg \rightarrow H$ to α_s

variation, since $gg \rightarrow H$ production via fermion triangle is proportional to α_S^2 even at LO, while $b\bar{b} \rightarrow H$ production at LO does not formally depend on α_S at all.

7 Conclusion

The standard CTEQ6 PDFs assume $\alpha_s(m_Z) = 0.118$. The PDFs presented here, constructed with other values for $\alpha_s(m_Z)$, can be used to find the range of uncertainty in predictions due to the uncertainty in $\alpha_s(m_Z)$.

We find that the standard fits with $\alpha_s(m_Z) = 0.118$ are adequate for many processes, because the uncertainty associated with $\alpha_s(m_Z)$ is smaller than the other sources of PDF uncertainty. However, the $\alpha_s(m_Z)$ uncertainty may be important for predictions that are sensitive to the gluon distribution, as shown in Fig. 2.

These fits can also be used to study the constraints from global fitting on the value of $\alpha_s(m_Z)$.

The CTEQ6 α_s -series of PDFs will be made available at the URL <http://cteq.org>, and at the standard LHAPDF archive <http://www-spines.dur.ac.uk/HEPDATA/>.

References

- [1] J. Pumplin, D.R. Stump, J. Huston, H.L. Lai, P. Nadolsky, W.K. Tung, JHEP 0207 (2002) 012 [hep-ph/0201195].
- [2] W.A. Bardeen, A.J. Buras, D.W. Duke and T. Muta, Phys. Rev. D18 3998 (1978).
- [3] Available at the web site www.nikhef.nl/h24/qcdnum.
- [4] J. Huston, J. Pumplin, D. Stump, W.K. Tung, JHEP 0506 (2005) 080 [hep-ph/0502080].
- [5] A.D. Martin, R.G. Roberts, W.J. Stirling, R.S. Thorne, Eur.Phys.J. C28 (2003) 455.
- [6] A. D. Martin, R. G. Roberts, W. J. Stirling and R. S. Thorne, Eur. Phys. J. C **23**, 73 (2002), [hep-ph/0110215].
- [7] D. Stump, J. Huston, J. Pumplin, W.K. Tung, H.L. Lai, S. Kuhlmann and J.F. Owens, JHEP 0310 (2003) 046 [hep-ph/0303013].
- [8] BCDMS Collaboration: A. C. Benvenuti *et al.*, Phys. Lett. **B223** (1989) 485; Phys. Lett. **B236** (1989) 592.
- [9] H1 Collaboration: C. Adloff *et al.*, Eur. Phys. J. **C13** (2000) 609; Eur. Phys. J. **C19** (2001) 269. Eur. Phys. J. **C21** (2001) 33.
- [10] ZEUS Collaboration: S. Chekanov *et al.*, Eur. Phys. J. **C21** (2001) 443.
- [11] NMC Collaboration: M. Arneodo *et al.*, Nucl. Phys. **B483** (1997) 3; and Nucl. Phys. **B487** (1997) 3.
- [12] CCFR Collaboration: U. K. Yang *et al.*, Phys. Rev. Lett. **86** (2001) 2742.

- [13] E866 Collaboration: R. S. Towell *et al.*, Phys. Rev. **D64** (2001) 052002.
- [14] CDF Collaboration: F. Abe *et al.*, Phys. Rev. Lett. **81** (1998) 5744.
- [15] CDF Collaboration: T. Affolder *et al.*, Phys. Rev. **D64** (2001) 032001.
- [16] D0 Collaboration: B. Abbott *et al.*, Phys. Rev. Lett. **86** (2001) 1707; and Phys. Rev. **D64** (2001) 032003.
- [17] Particle Data Group: S. Eidelman *et al.*, Phys. Lett. B592 (2004) 1.
- [18] J. Pumplin *et al.*, Phys. Rev. **D65** (2002) 014013 [hep-ph/0101032].
- [19] ZEUS Collaboration: S. Chekanov *et al.*, Phys. Rev. D67, 012007 (2003).
- [20] MISSING: HERA alpha (+gluon) determinations.
- [21] MISSING: CDF alpha determinations – get from Joey.
- [22] M. Spira, A. Djouadi, D. Graudenz and P. M. Zerwas, Nucl. Phys. B **453**, 17 (1995) [arXiv:hep-ph/9504378].
- [23] M. Spira, Nucl. Instrum. Meth. A **389**, 357 (1997) [arXiv:hep-ph/9610350].
- [24] C. Balazs, H. J. He and C. P. Yuan, Phys. Rev. D **60**, 114001 (1999) [arXiv:hep-ph/9812263].
- [25] A. Djouadi and S. Ferrag, Phys. Lett. B **586**, 345 (2004), [hep-ph/0310209].
- [26] A. Belyaev, J. Pumplin, W. K. Tung and C. P. Yuan, [hep-ph/0508222].
- [27] Z. Sullivan and P. M. Nadolsky, in *Proc. of the APS/DPF/DPB Summer Study on the Future of Particle Physics (Snowmass 2001)* ed. N. Graf, eConf **C010630**, P511 (2001) [arXiv:hep-ph/0111358].
- [28] A. Belyaev, J. Pumplin, W. K. Tung and C. P. Yuan, arXiv:hep-ph/0508222.